Available online at www.sciencedirect.com
ScienceDirect
Catalysis Today 125 (2007) 97–102
CATALYSIS TODAY
www.elsevier.com/locate/cattod

Methanol oxidation reforming over a $ZnO\text{-}Cr_2O_3/CeO_2\text{-}ZrO_2/Al_2O_3$ catalyst in a monolithic reactor

Guangwen Chen *, Shulian Li, Hengqiang Li, Fengjun Jiao, Quan Yuan

Dalian Institute of Chemical Physics, Chinese Academy of Sciences, 457 Zhongshan Road, Dalian 116023, China

Available online 27 April 2007

Abstract

Catalysts with a high activity and a high stability play an important role in the process of hydrogen generation via methanol oxidation reforming for PEM fuel cell. In this paper, catalysts with high activities and selectivities for methanol oxidation reforming have been developed. The reaction experimental results indicate that a $ZnO\text{-}Cr_2O_3/CeO_2\text{-}ZrO_2/Al_2O_3$ ceramic monolithic catalyst is a promising catalyst for the hydrogen production from methanol oxidation reforming. There was no significant deactivation of the catalyst over 1000 h of continuous operation and the CO concentration in the reformate effluent dry gas was less than 1.4%, and methane produced was negligible under the molar ratios of O_2/MeOH = 0.3, H_2O/MeOH = 1.2, and gas hourly space velocity equal to 3850 h^{-1}.

Keywords: Methanol autothermal reforming; Monolithic catalyst; Microchannel reactor; Microstructured reactor; Wall coating

1. Introduction

Automotive exhaust is currently one of the major pollution sources in cities. As a pollution-free and energy-saving power supply for electric vehicles, the fuel cell is the best candidate due to its high energy conversion efficiency (50–70%) and zero or nearly zero emission. Proton exchange membrane fuel cell (PEMFC) is the most promising fuel cell and hydrogen is the fuel for PEMFC. However, the storage and handling of on-board hydrogen in the fuel cell vehicles is still an unsolved issue. One of the solutions is to use hydrocarbon fuels as hydrogen carrier. Among all possible choices of fuels, the on-board generation of hydrogen from methanol is known as one of the most practical ways for proton exchange membrane (PEM) fuel cells vehicle due to its high ratio of hydrogen to carbon and low reaction temperatures [1]. However, the miniaturization of hydrogen source is the prerequisite for its practical application [2,3].

The on-board fuel processor will require novel catalysts and reactor configurations. The technologies of converting methanol into a hydrogen-rich supply for the fuel cells are mainly based on steam reforming, partial oxidation, or a combination of both, namely oxidation steam reforming, oxidation reforming, or autothermal reforming. For the sake of energy savings, fast start-up, and quick response of the whole system, methanol oxidation reforming is the most promising way. This process has a net reaction enthalpy change of zero, and thus a reactor for this process does not require any extra external heat after the reaction temperature is attained [4]. Due to thermodynamic constraints of methanol reforming, significant amount of CO, as a poisoning impurity of platinum electro-catalyst, will be produced. It is also necessary to reduce the level of CO in the hydrogen-rich gas to less than 50 ppm, even though high CO-resistant electro-catalysts were developed. So the process of a preferential oxidation of CO (PROX) is required [5].

With the great progresses achieved in the new area of microreactor technology [6–8], it is now feasible to use microchannel reactors in the field of on-board PEMFC hydrogen sources via methanol conversion [9,10]. Microchannel reactors favor isothermal operating conditions due to its high surface-to-volume ratio, enhanced heat and mass transfer, and intrinsic safety. The application of microreaction technology can greatly improve the efficiency of systems and diminish their volumes and weights. However, it is still a challenging task to prepare catalysts with high activities and stabilities coated onto the walls of the microchannels [11–13] and to avoid heavily heat losses in the microreactors [14].

* Corresponding author. Tel.: +86 411 437 9031; fax: +86 411 469 1570.
E-mail address: gwchen@dicp.ac.cn (G. Chen).

0920-5861/$ – see front matter © 2007 Elsevier B.V. All rights reserved.
doi:10.1016/j.cattod.2007.03.049

Structured monolithic catalysts have been widely applied in automotive emission control systems [15–18]. Recently, other applications on the chemical industry [19–21] and especially the hydrogen generation from methanol [22–25] have also been of much interest because of the unique features of monoliths, such as low pressure drop, low radial heat flow, uniform flow and rapid mass transport. Because the radial heat transfer occurs only by conduction through the laminar flow and the solid walls, the reaction in the ceramic monolithic reactor can be performed as nearly an adiabatic process. Therefore, the ceramic monolithic reactor is one of the best candidates for the methanol autothermal reforming reactions.

The current investigations of hydrogen production from methanol mainly focus on Cu-based, Pt-based and Pd-Zn catalysts [11,26–28]. However, Cu-based catalysts deactivate quickly and Pt-based catalyst has poor selectivity. Pd-Zn catalysts are extremely expensive, though they have a high activity and selectivity. Hence, they are not suitable for on-board production of hydrogen. It is well known that $ZnO\text{-}Cr_2O_3$ catalysts have been used for hydrocarbon synthesis from synthesis gas [29,30]. Our studies also showed that $ZnO\text{-}Cr_2O_3$ catalysts are promising catalysts for the hydrogen production from methanol [31,32].

The objective of this study is to develop a micro fuel processor with $ZnO\text{-}Cr_2O_3/CeO_2\text{-}ZrO_2/Al_2O_3$ ceramic monolithic catalyst for methanol oxidation reforming. Both the performances of the catalyst and process behaviors of the microstructured reactor for methanol oxidation reforming reactions are investigated experimentally in detail.

2. Experimental

2.1. Catalyst preparation

The samples of cordierite honeycomb ceramic with 400 cpsi (cells per square inch, cpsi) were used as the substrate in this work. The height, diameter and volume of samples are 22 mm, 16 mm and 4.5 mL, respectively, and the diameter of channel is 1 mm.

$ZnO\text{-}Cr_2O_3/CeO_2\text{-}ZrO_2/Al_2O_3$ monolithic catalysts for methanol oxidation reforming developed by our lab were made up of two layers, i.e., the wash-coating layer of $\gamma\text{-}Al_2O_3$ and active layer of $ZnO\text{-}Cr_2O_3/CeO_2\text{-}ZrO_2$. The wash-coating layer of $\gamma\text{-}Al_2O_3$ is coated on the honeycomb ceramic substrate as the supporting layer of the catalytic activity component. Activity components and promoters of the $ZnO\text{-}Cr_2O_3/CeO_2\text{-}ZrO_2$ catalysts are then coated onto the supporting coat to prepare the methanol oxidation reforming hydrogen production catalyst.

The wash-coating layer of $\gamma\text{-}Al_2O_3$ was prepared by a sol–gel process, then dried at room temperature for 12 h and at 393 K for 6 h, and calcined in air at 773 K for 4 h. Then, the honeycomb ceramic substrate with $\gamma\text{-}Al_2O_3$ layer was impregnated by nitric acid solution of $Ce(NO_3)_3{\cdot}6H_2O$ and $Zr(NO_3)_4{\cdot}5H_2O$ (CeO_2:ZrO_2 = 4:1 in weight ratio, Shanghai Yuelong Chemical Company). The impregnated sample was then dried in air and calcined at 500 °C for 4 h. The calcined sample was further impregnated by nitric acid solution of $Zn(NO_3)_2{\cdot}6H_2O$ and $Cr(NO_3)_3{\cdot}9H_2O$ (ZnO:Cr_2O_3 = 4:1 in weight ratio, Shanghai Chemical Company) and was then dried in air. The $ZnO\text{-}Cr_2O_3/CeO_2\text{-}ZrO_2/Al_2O_3$ ceramic monolithic catalyst was finally formed after calcined at 500 °C for 4 h. The weight ratios of $ZnO\text{-}Cr_2O_3$, $CeO_2\text{-}ZrO_2$, $\gamma\text{-}Al_2O_3$ layers in the catalyst samples were 6, 8 and 15%, respectively.

2.2. Experimental procedures and analysis method

The methanol oxidation reforming was carried out in a fixed-bed flow reaction system with ceramic monolithic catalyst at atmospheric pressure in a tubular quartz reactor (18 mm i.d.) inside an electric furnace. The monolithic catalyst was sealed in the reactor by silica alumina cloth. To measure the reaction temperature, a thermocouple with a diameter of 0.5 mm was inserted through the back of ceramic monolith catalyst along the center channel and was fixed at the point with a distance of 3 mm from the front of catalyst. The thermocouple can also be inserted at different positions, such as A, B and C (shown in Fig. 1), and can be easily moved along the axis of the channel to measure the reaction temperature distribution. Prior to the reaction, the catalyst was reduced in situ in a stream of 10% H_2 in N_2 (50 mL/min) at 400 °C for 2 h. The mixture of liquid methanol (>99.5% purity) and water was pumped into a vaporizer kept at 200 °C by a precise P230 constant flow pump (Dalian Elite Analytical Instruments Company) and conveyed into the reactor by air as carrier gas and oxidant, while N_2 in air as internal standard for product analysis. The air flow rate was precisely controlled by mass flow controllers. The reaction temperature inside the monolithic catalyst was controlled in the range of 280–340 °C, and the gas hourly space velocity (GHSV) was kept at 2000–12,000 h^{-1}. A schematic sketch of the testing system setup is similar with the article [33] except for the different reactors.

The effluent of the reactor consisted of H_2, CO_2, CO, CH_4 and N_2 as well as H_2O and/or methanol, but the concentration of CH_4 in the effluent is negligible during the experiments. After the reaction, the product gases were passed through a cold trap (mixture of ice and water) and a dryer to remove water and methanol, and the dry gas entered an on-line gas chromatograph (GC4000A, Beijing East & West Analytical Instruments Inc.)

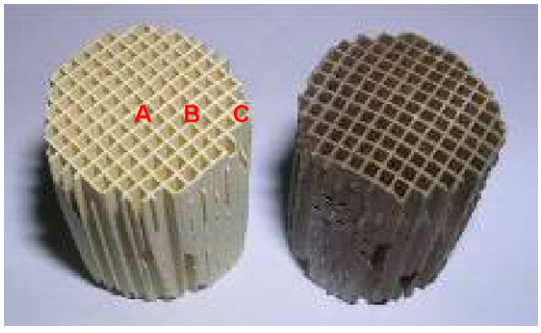

Fig. 1. The samples of cordierite honeycomb ceramic substrate and catalyst used with 400 cpsi. Temperature measure point: (A) center; (B) middle; (C) outer layer.

equipped with TCD detector for analyzing the composition. A carbon molecular sieve column was used to analyze the dry gaseous components. The flow rate of the dry gaseous products was measured by a soap bubble flow meter [34].

In this paper, gas hourly space velocity is defined as the ratio of feed volumetric flow rate of methanol to the monolithic catalyst volume (4.5 mL). Methanol conversion (X_{MeOH}) and product yields are calculated based on the flow rate and compositions of the dry gaseous products based on the carbon balance, and can be written as following:

$$X_{MeOH} = \frac{F(y_{CO} + y_{CO_2} + y_{CH_4})}{22.4 \times n^0_{MeOH}} \times 100\% \quad (1)$$

where F is referred as the normal volumetric flow of dry reformate gas, mL(STP)/min, n^0_{MeOH} is defined as the molar flow rate of methanol in feed, mmol/min, and y_{CO}, y_{CO_2} and y_{CH_4} are defined as the molar compositions of CO, CO_2 and CH_4 in dry reformate gas, respectively.

In order to eliminate the errors caused by catalyst deactivation, all the data were collected when the catalytic activity was stable, and the data of each reaction condition were repeated three times. Material balances on N_2 were calculated to verify the measurement accuracy. In this work, the relative error of the N_2 flow rate in feed and dry effluent is less than 3%.

3. Results and discussion

3.1. Effects of O_2/MeOH and H_2O/MeOH molar ratios

Methanol autothermal reforming reaction (ATR) has a net reaction enthalpy change of zero which is a combination of the endothermic steam-reforming reaction and the exothermic partial oxidation reaction, thus a reactor for this process does not require any extra external heat after having attained reaction temperature. The molar ratio of oxygen to methanol, β, varies with different reaction temperatures, reaction pressure, feed composition and other factors as well. Table 1 shows β under adiabatic reaction conditions with a stoichiometric ratio, where β increases with the temperature increase.

$$CH_3OH + (1 - 2\beta)H_2O + \beta O_2 \rightarrow CO_2 + (3 - 2\beta)H_2 \quad (2)$$

Due to the higher molar ratio of the adopted H_2O/MeOH and the heat dissipation to the environment, the molar ratio of oxygen to methanol must be somewhat higher than the stoichiometric one as to maintain the reaction. When air and pure oxygen were used as the oxidants, the highest hydrogen concentration, $C_{H_2,max}$, in the reformate dry gas can be calculated via the following formula, respectively, and the results are shown in Table 2.

$$C_{H_2,max} = \frac{3 - 2\beta}{4 + (79.1/20.9 - 2)\beta} \times 100\% \approx \frac{3 - 2\beta}{4 + 1.785\beta} \times 100\% \quad (3)$$

$$C_{H_2,max} = \frac{3 - 2\beta}{4 - 2\beta} \times 100\% \quad (4)$$

The methanol conversions, H_2, CO_2 and CO concentrations in the reformate effluent dry gas on the ZnO-Cr_2O_3/CeO_2-ZrO_2/Al_2O_3 ceramic monolithic catalyst with the O_2/MeOH and H_2O/MeOH molar ratios are shown in Figs. 2 and 3, respectively. The methanol conversion increased from 83.8 to 98.7% with the increase of the O_2/MeOH molar ratio from 0.20 to 0.225 as shown in Fig. 2, and it reached at nearly 100% when the O_2/MeOH molar ratio was higher than 0.25 under the reaction conditions. The results in Fig. 3 show that the O_2/MeOH molar ratio should be increased in order to keep the same methanol conversion at higher H_2O/MeOH molar ratio. CO and H_2 concentrations were not evidently changed with different H_2O/MeOH and O_2/MeOH molar ratios, while the H_2 concentration varied with O_2/MeOH molar ratios. CO was the main by-product formed in the reforming process, and its concentration in the reformate dry gas was in the ranges of 1.15–1.25%, which was far lower than the balanced stoichiometric concentration of the WGS, suggesting that CO cannot be a reaction intermediate. So CO can be directly removed via preferential oxidation, and a process of water–gas shifting was no more necessary for this system.

3.2. Effects of reactor control temperature and GHSV

The effects of GHSV and reactor control temperatures (light-off temperature) on the methanol conversions, H_2 and CO concentrations in reformate effluent dry gas on the ceramic monolithic catalyst are shown in Figs. 4 and 5, respectively. In Fig. 4, the methanol conversion rapidly increases with

Table 1
Effect of reaction temperature on β under stoichiometric reaction

T (°C)	300	400	500	600	700
β	0.123	0.129	0.133	0.137	0.140

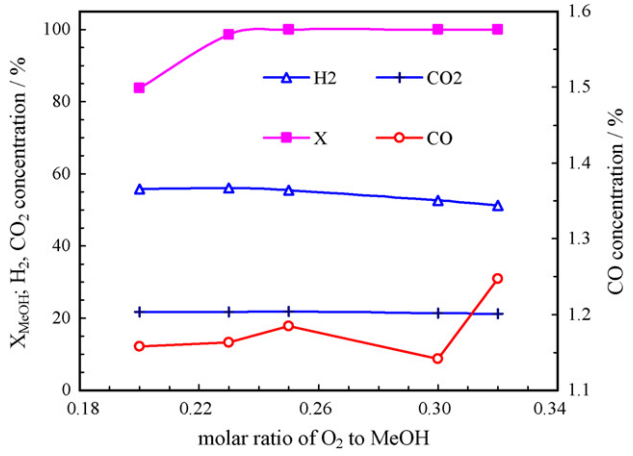

Fig. 2. Product distribution for methanol oxidation reforming vs. molar ratio of O_2 to MeoH. GHSV = 3850 h^{-1}, H_2O/MeOH = 1.2 (molar ratio), reactor control temperature T = 280 °C.

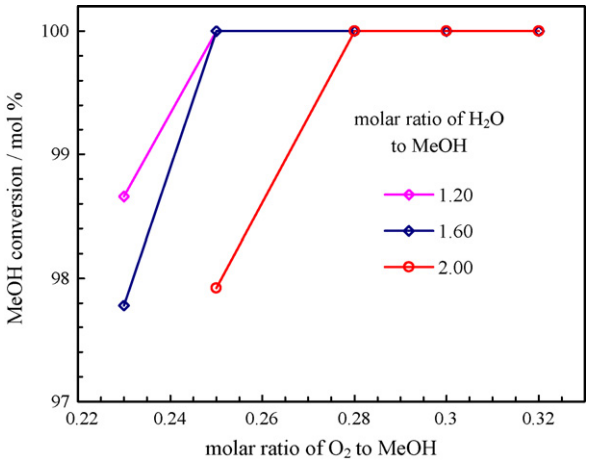

Fig. 3. Methanol conversion for methanol oxidation reforming vs. molar ratio of O_2 to MeOH under different molar ratio of H_2O to MeOH. GHSV = 3850 h^{-1}, reactor control temperature T = 280 °C.

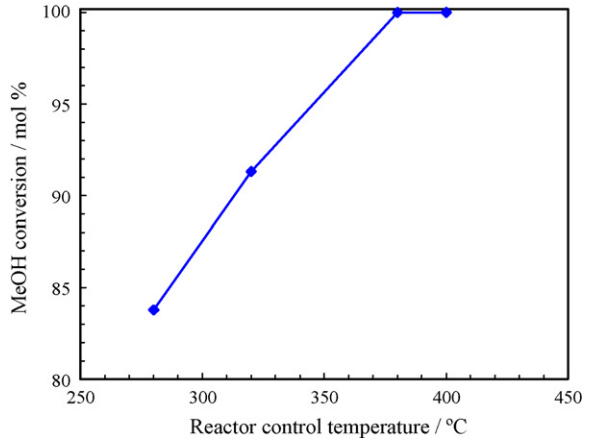

Fig. 4. Methanol conversion vs. reactor control temperature under O_2/MeOH = 0.2. O_2/MeOH = 0.2, H_2O/MeOH = 1.2 (molar ratio), GHSV = 3850 h^{-1}.

increasing reactor control temperature under the reaction conditions of O_2/MeOH = 0.2, H_2O/MeOH = 1.2 and GHSV = 3850 h^{-1}. The MeOH conversion is 83.8 and 91.3% at 280 and 320 °C, respectively. Above 380 °C, the conversion was nearly 100%. Due to the heat of the reactor system dissipated to the environment, in order to maintain the reaction process and acquire the same methanol conversion, the lower the O_2/MeOH molar ratio and the higher GHSV, the higher the reactor control temperature (corresponding to the reaction light-off temperature) was needed. If a 100% methanol conversions is required, the reactor control temperature should be kept at 280 °C for GHSV < 7000 h^{-1}, 300 °C for GHSV = 7700 h^{-1}, or 340 °C for GHSV = 11,500 h^{-1} as shown in Fig. 5, respectively.

Table 2
The highest H_2 concentration (mol%) in reformate dry gas under different β and oxidants

β	0.175	0.2	0.225	0.25	0.275	0.3	0.325
Air	61.45	59.67	57.93	56.23	54.56	52.92	51.31
O_2	72.60	72.22	71.83	71.43	71.01	70.59	70.15

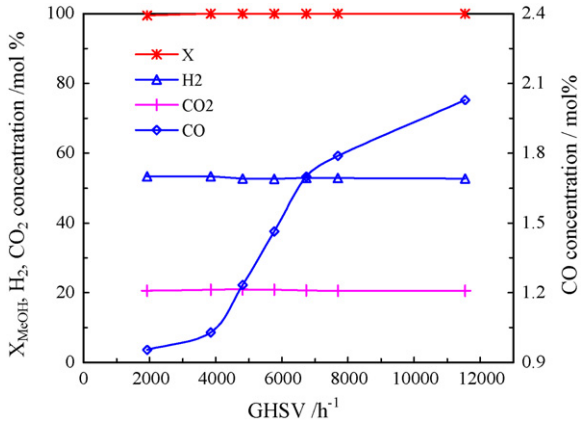

Fig. 5. Methanol conversion and product distribution for methanol oxidation reforming under different gas hourly space velocity. O_2/MeOH = 0.3, H_2O/MeOH = 1.2 (molar ratio); reactor control temperature T = 280 °C for GHSV < 7000 h^{-1}, 300 °C for GHSV = 7700 h^{-1}, 340 °C for GHSV = 11,500 h^{-1}.

The H_2 concentration decreased slightly as the GHSV increased, while the CO concentration increased distinctly as GHSV increased. The results in our early work [31,32,35] indicated that the major pathway of CO formation in the steam reforming was through the reaction of methanol decomposition without the WGS reaction. The methanol decomposition reaction competed with the main reaction of methanol oxidation reforming in parallel. The activation energy of the former was greater than the later, so a higher temperature in the catalyst bed with higher GHSVs favors the CO formation (shown in Fig. 5). Meanwhile, CO cannot be converted completely into CO_2 due to the low residence time.

3.3. Temperature distribution of catalyst bed

Figs. 6–8 showed the temperature distribution of monolithic catalyst bed under different radial distance (shown in Fig. 1), molar ratio of O_2 to MeOH and GHSV. The perfect adiabatic

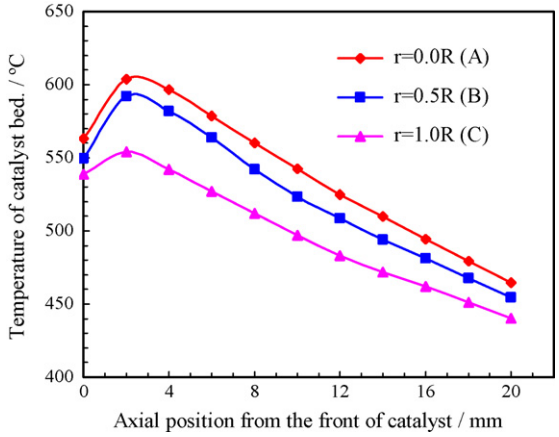

Fig. 6. Axial temperature distribution of catalyst bed under different radial distances from center. O_2/MeOH = 0.3, H_2O/MeOH = 1.2 (molar ratio), GHSV=3850 h^{-1}, control temperature T = 280 °C.

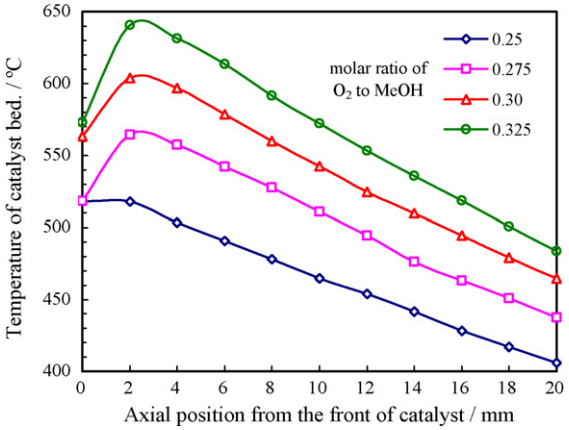

Fig. 7. Axial temperature distribution of catalyst bed in the center. H_2O/MeOH = 1.2 (molar ratio), GHSV=3850 h^{-1}, reactor control temperature T = 280 °C.

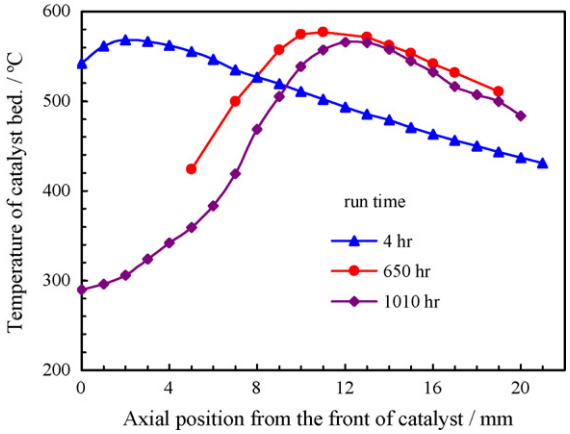

Fig. 9. Axial temperature distribution of catalyst bed in the center. O_2/MeOH = 0.3, H_2O/MeOH = 1.2 (molar ratio), GHSV=3850 h^{-1}, control temperature T = 280 °C.

process cannot be realized due to the heat dissipation of the reactor to the environment, so a radial temperature gradient is present in the catalyst bed. The temperature differences between the center (A) and side (C) were in the ranges of 25–50 °C as shown in Fig. 6. The temperature in the catalyst bed was higher when the molar ratio of O_2 to MeOH and GHSV increased as shown in Figs. 7 and 8. Form these figures, we found that the location of the highest temperature for this fresh monolithic catalyst was identical, i.e., 2.0 mm from the front surface of the catalyst. The position of the temperature peak shifted backward along the axis of the reaction channel with the increase of run time as shown in Fig. 9. The displacement rate of the temperature peak was nearly in linear versus the running time, and the lift time of the catalyst can be easily determined by this phenomena. The reason for the catalyst deactivation can be ascribed to sintering and volatilization of the active component, Zn.

According to the kinetics study, there were two temperature zones in the catalyst bed. Methanol oxidation and decomposition reactions will happen in the first zone in front of temperature peak, while, the methanol steam reforming will happen in the second zone after temperature peak.

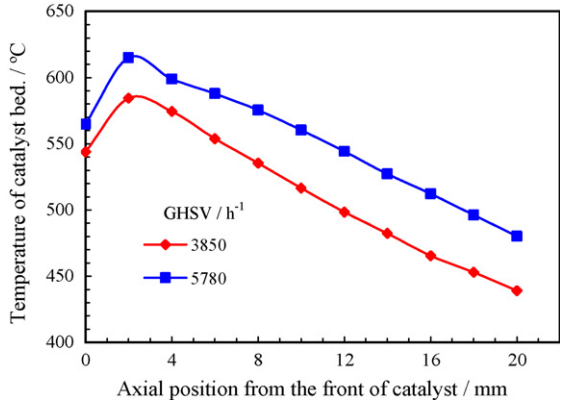

Fig. 8. Axial temperature distribution of catalyst bed in the center. O_2/MeOH = 0.3, H_2O/MeOH = 1.2 (molar ratio), reactor control temperature T = 280 °C.

3.4. Stability test for monolithic catalyst

The stability of $ZnO\text{-}Cr_2O_3/CeO_2\text{-}ZrO_2/Al_2O_3$ ceramic monolithic catalyst was evaluated by running for 1000 h under the reaction conditions of O_2/MeOH = 0.3, H_2O/MeOH = 1.2 and GHSV = 3850 h^{-1}. The results in Fig. 10 indicate that the catalyst had a high activity and stability and a low CO selectivity. The methanol conversion was nearly 100%, the CO concentration in the product was lower than 1.4 mol%, and the H_2 concentration was nearly constant during the 1000 h test. This catalyst showed a higher thermal stability than Cu-based catalysts, and it can be explained by that the thermal resistance of $ZnO\text{-}Cr_2O_3$ is superior to that of Cu that easily sinters at high temperatures. Studies have shown that the introduction of ZrO_2 into the ceria lattice significantly increases the oxygen species storage capacity [36–38] and thermal resistance [17,39] owing to the formation of a solid solution. Additionally, the results reported by Agrell et al. [40] showed that catalysts containing ZrO_2/Al_2O_3 were highly resistant to redox cycles and exhibit a high stability. These factors probably helped to improve the stability of the catalyst.

The product gas dry flow rate was 80 L/h at GHSV of 3850 h^{-1}, among which 42 L/h was hydrogen. So the process

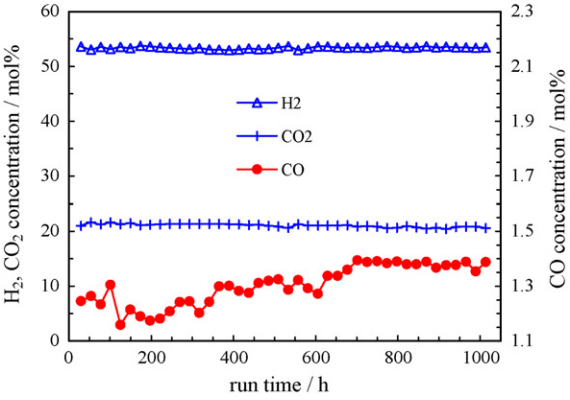

Fig. 10. 1000 h test of the catalyst stability. O_2/MeOH = 0.3, H_2O/MeOH = 1.2 (molar ratio), GHSV=3850 h^{-1}, control temperature T = 280 °C.

was able to support a PEM fuel cell of 70 W based on 600 L(H_2)/h/kW.

4. Conclusion

The non-noble metal oxides of ZnO-Cr_2O_3/CeO_2-ZrO_2/Al_2O_3 in monolithic catalysts developed for methanol oxidation reforming had high activities and long-term stabilities during the experiment for more than 1000 h. CH_3OH conversion was close to 100% and the CO content in the reformate dry gas was lower than 1.4%, so the water–gas shifting process becomes unnecessary for the system with monolithic catalysts for methanol oxidation reforming. The developed fuel processor generates enough hydrogen for power output of 70 W with the monolithic catalyst volume of 4.5 mL.

Given the small characteristic dimensions and the high performance of heat insulation of monolithic reactors, the reaction can be carried out in an autothermal state when the reaction is lighted-off. From this point, the structured monolithic catalyst is an excellent candidate for the process of autothermal reforming. For the future, how to integrate the sub-processes, i.e., methanol autothermal reforming, CO PROX, combustion, vaporization and micro-heat exchanger, into a whole system of PEM fuel cell with higher efficiency for practical applications, is still a challenging task.

Acknowledgements

We gratefully acknowledge the financial supports for this project from National Natural Science Foundation of China and China National Petroleum Corporation (No. 20176057, No. 20122201 and No. 20490208), Key Program for International Cooperation of Science and Technology (No. 2001CB711203).

References

[1] R.L. Borup, M.A. Inbody, T.A. Semelsberger, J.I. Tafoya, D.R. Guidry, Catal. Today 99 (2005) 263.
[2] Y. Choi, H.G. Stenger, Appl. Catal. B 38 (2002) 259.
[3] A.Y. Tonkovich, J.L. Zilka, M.J. Lamont, Y. Wang, R.S. Wegeng, Chem. Eng. Sci. 54 (1999) 2947.
[4] G.W. Chen, Q. Yuan, S.L. Li, Chin. J. Catal. 23 (2002) 491.
[5] G.W. Chen, Q. Yuan, H.Q. Li, S.L. Li, Chem. Eng. J. 101 (2004) 101.
[6] K. Jähnisch, V. Hessel, H. Löwe, M. Baerns, Angew. Chem. Int. Ed. 43 (2004) 406.
[7] G. Kolb, V. Hessel, Chem. Eng. J. 98 (2004) 1.
[8] Y.C. Zhao, G.W. Chen, Q. Yuan, AIChE J. 52 (2006) 4052.
[9] J.D. Holladay, Y. Wang, E. Jones, Chem. Rev. 104 (2004) 4767.
[10] C. Tsouris, J.V. Porcelli, Chem. Eng. Prog. 99 (10) (2003) 50.
[11] P. Pfeifer, K. Schubert, G. Emig, Appl. Catal. A 286 (2005) 175.
[12] J. Kobayashi, Y. Mori, K. Okamoto, R. Akiyama, M. Ueno, T. Kitamori, S. Kobayashi, Science 304 (2004) 1305.
[13] M.T. Janicke, H. Kestenbaum, U. Hagendorf, F. Schüth, M. Fichtner, K. Schuberty, J. Catal. 191 (2000) 282.
[14] J.Y. Won, H.K. Jun, M.K. Jeon, S.I. Woo, Catal. Today 111 (2006) 158.
[15] P. Forzatti, D. Ballardini, L. Sighicelli, Catal. Today 41 (1998) 87.
[16] M. Shelef, R.W. McCabe, Catal. Today 62 (2000) 35.
[17] S.L. Li, G.W. Chen, J.L. Sun, H.Q. Li, Chin. J. Catal. 23 (2002) 341.
[18] E.C. Su, C.N. Montreuil, W.G. Rothschild, Appl. Catal. 17 (1985) 65.
[19] A. Cybulski, J.A. Moulijn, Catal. Rev.-Sci. Eng. 36 (1994) 179.
[20] S. Irandoust, B. Andersson, Catal. Rev.-Sci. Eng. 30 (1988) 341.
[21] A. Stankiewicz, Chem. Eng. Sci. 56 (2001) 359.
[22] B.E. Traxel, K.L. Hohn, Appl. Catal. A: Gen. 244 (2003) 129.
[23] M. Schuessler, M. Portscher, U. Limbeck, Catal. Today 79–80 (2003) 511.
[24] B. Lindström, J. Agrell, L.J. Pettersson, Chem. Eng. J. 93 (2003) 91.
[25] C.M. Mitchell, D.P. Kim, P.J.A. Kenis, J. Catal. 241 (2006) 235.
[26] C. Cao, G. Xia, J. Holladay, E. Jones, Y. Wang, Appl. Catal. A 262 (2004) 19.
[27] H. Purnama, T. Ressler, R.E. Jentoft, H. Soerijanto, R. Schlögl, R. Schomäcker, Appl. Catal. A 259 (2004) 83.
[28] S. Liu, K. Takahashi, K. Uematsu, M. Ayabe, Appl. Catal. A: Gen. 283 (2005) 125.
[29] F. Simard, U.A. Sedran, J. Sepúlveda, N.S. Fígoli, H.I. de Lasa, Appl. Catal. A 125 (1995) 81.
[30] M.C.J. Bradford, M.V. Konduru, D.X. Fuentes, Fuel Process. Technol. 83 (2003) 11.
[31] W.Q. Cao, G.W. Chen, S.L. Li, Q. Yuan, Chem. Eng. J. 119 (2006) 93.
[32] W.Q. Cao, G.W. Chen, J.S. Chu, S.L. Li, Q. Yuan, Chinese J. Catal. 27 (2006) 895.
[33] G.W. Chen, S.L. Li, Q. Yuan, Catal. Today 120 (2007) 63.
[34] S.L. Li, G.W. Chen, F.J. Jiao, H.Q. Li, Chin. J. Catal. 25 (12) (2004) 979.
[35] W.Q. Cao, Thesis for master degree, Dalian Institute of Chemical Physics, Chinese Academy of Sciences, Dalian, 2006.
[36] C.E. Hori, H. Permana, K.Y.S. Ng, A. Brenner, K. More, K.M. Rahmoeller, D. Belton, Appl. Catal. B 16 (1998) 105.
[37] H. Vidal, S. Bernal, J. Kašpar, M. Pijolat, V. Perrichon, G. Blanco, J.M. Pintado, R.T. Baker, G. Colon, F. Fally, Catal. Today 54 (1999) 93.
[38] P. Fornasiero, E. Fonda, R. Di Monte, G. Vlaic, J. Kašpar, M. Graziani, J. Catal. 187 (1999) 177.
[39] F. Fally, V. Perrichon, H. Vidal, J. Kaspar, G. Blanco, J.M. Pintado, S. Bernal, G. Colon, M. Daturi, J.C. Lavalley, Catal. Today 59 (2000) 373.
[40] J. Agrell, H. Birgersson, M. Boutonnet, I. Melián-Cabrera, R.M. Navarro, J.L.G. Fierro, J. Catal. 219 (2003) 389.